Early dynamics of the potential energy evolution in two-dimensional gas-liquid phase

separation

Early dynamics of the potential energy evolution in two-dimensional gas–liquid phase separation

Sheng-You Huang, Xian-Wu Zou[1] and Zhun-Zhi Jin

Department of Physics, Wuhan University, Wuhan 430072, People's Republic of China

E-mail: xwzou@whu.edu.cn (Xian-Wu Zou)

Abstract
Molecular dynamics simulations have been performed to investigate the early-time dynamic behaviour of gas–liquid phase separation in two dimensions by using the evolution of the potential energy. It is found that the average potential energy per particle $u(t)$ shows a good linear relationship with the average number of nearest-neighbour particles $n_{nn}(t)$ after a brief time. The results also show that $u(t)$ follows a positive power law in time in the early stage of phase separation. The excess energy per particle $u(t) - u_\infty \propto t^{-1/2}$ is also confirmed in the late stage. These results suggest that $u(t)$ may be considered as a parameter describing the entire phase separation process in gas–liquid systems.

1. Introduction

The phenomenon of phase separation has been extensively studied both experimentally and theoretically, in a wide variety of systems, including simple fluids, binary fluids, binary alloys, and magnetic systems [1–12]. It has been shown that in the late stage of phase separation the typical domain size $R(t)$ grows as a power law with time t [13]:

$$R(t) \sim t^\alpha. \tag{1}$$

The exponent α is believed to be universal, depending on the growth mechanism rather than details of the particular system.

Lifshitz and Slyozov have analysed the dynamics of aggregation of solutes from super-saturated dilute solutions using a scaling concept [14]. They found that the late-time behaviour of the growth law of the solute domain is the scaling $R(t) \sim t^{1/3}$. Recently, by using dimensional analysis, Lookman *et al* [15] have found that there are three dynamic regimes: diffusive, viscous, and inertial. In the diffusive regime, the diffusion order parameter plays a main role and $R(t) \sim t^{1/3}$. In the viscous regime, hydrodynamics becomes relevant

---

[1] Author to whom any correspondence should be addressed.

and $R(t) \sim t$. In the inertial regime, inertial effects dominate over the viscous forces and $R(t) \sim t^{2/3}$.

Numerical studies have also been made of phase separation by Monte Carlo simulation, lattice Boltzmann simulation, and solving phenomenological equations [16–20]. It is found that the growth exponent α is equal to $1/2$ for the case of non-conserved order parameter and $1/3$ for the case of conserved order parameter. In the late stage of phase separation, the temporal patterns are statistically equivalent to each other if they are scaled by the proper time-dependent characteristic length. The influences of density and noise on phase separation dynamics have also been studied by our group recently using molecular dynamics (MD) simulations [21]. The simulations indicate that in the late stage of gas–liquid phase separation, the mean cluster size $R(t) \sim t^\alpha$ with $\alpha = 1/3$ (for low density and high temperature) or $1/2$ (for the rest) [21]. Koch *et al* [22] have studied the influence of the ensemble on gas–liquid phase separation in a two-dimensional (2D) Lennard-Jones (LJ) fluid at the critical density ρ_c. They have found that the characteristic length scale of the system grows in proportion to $t^{1/2}$ for the isothermal simulation and to $t^{1/3}$ for the adiabatic one. Yamamoto and Nakanishi [23] also studied the dynamics of gas–liquid phase separation in the two- and three-dimensional LJ fluid systems with critical density by means of constant-temperature MD. They found that the growth exponent is $1/2$ and is independent of the system dimensionality. Another important finding from MD simulation is that the domain pattern undergoing phase separation shows a fractal nature under certain conditions [24, 25]. It has also been found that the fractal dimension of the domain wall increases with rising temperature [23]. Such fractal behaviour was also predicted analytically by Klein [26] using scaling in the early stage of the spinodal decomposition. MD simulation has the advantage that both static and dynamic correlation and hydrodynamic effects are all taken into consideration. It has also been carried out for the binary fluid mixture [27–32].

However, most of the works mentioned above considered the late-time behaviours of phase separation, and they were focused on the growth of the characteristic length. The early-time behaviours of phase separation have received rather little attention as far as we are aware, especially for an unstable fluid which still presents a major unsolved problem in the dynamics of first-order phase separation [1, 2]. In this paper, we aimed to obtain some deeper understanding of the phase separation process by studying the early-time behaviours of gas–liquid separation. The dynamic behaviour of systems is characterized by using the average potential energy per particle. The relationship between the potential energy and pair distribution function, and the evolution of the potential energy with time were obtained. The early-time dynamic behaviours of gas–liquid phase separation were first studied, and the long-time behaviours were also confirmed.

2. Model and method

We have simulated the spinodal decomposition and cluster growth of a 2D simple fluid by means of molecular dynamics. The system consists of $N = 5000$ particles with mass m. The interaction between two particles separated by distance r is described using the Lennard-Jones potential

$$\phi(r) = 4\varepsilon \left[\left(\frac{\sigma}{r} \right)^{12} - \left(\frac{\sigma}{r} \right)^6 \right] \tag{2}$$

where ε denotes the potential depth and σ is the diameter of a particle. Reduced units are used. ε, σ, ε/k_B, and $\tau = \sqrt{m\sigma^2/4\varepsilon}$ are chosen as the energy, length, temperature, and time units, respectively. The Boltzmann constant k_B and atomic mass m are set to 1. The MD time step (MDs) was taken as 0.01, which is equal to about 0.01 ps for an argon-like fluid. 20 000

time steps were taken in a MD run, to reach the late stage of phase separation. The MD runs were performed in the constant-*NVT* (constant number of particles, volume, and temperature) ensemble, where the temperature is fixed by a Nosé–Hoover thermostat [33]. The periodic boundary condition was used as usual. The cut-off radius was set at $r_{cut} = 3.0$.

For 2D LJ fluids, the critical density ρ_c and critical temperature T_c are 0.325 and 0.56, respectively [34]. The MD simulations were carried out by the instantaneous critical quenching of homogeneous systems. That is, the system was initially equilibrated at the critical density $\rho = 0.325$ and temperature $T = 5.0$, corresponding to the single-phase region in the phase diagram of the 2D LJ fluid. Then the system was quenched into the two-phase (spinodal) region by the instantaneous velocity scaling of all particles, while the density remained unchanged. To remove the fluctuation, at least ten independent runs were performed to average the calculated results.

In simulations, the definition of a cluster is almost the same as that used by Ten Wolde and Frenkel [5]. It can be given briefly as follows. A distinction is first made between particles that have a liquid-like environment and those that have a vapour-like environment. Two particles are defined as the nearest neighbours to each other if the distance between them is less than r_c, where $r_c = 1.6$ corresponds to the first minimum in the radial distribution function of the systems. The particles which have more than two nearest neighbours are considered to be liquid-like. Thus any two liquid-like particles which are separated by a distance less than r_c belong to the same liquid cluster.

3. Results and discussion

3.1. The relation between structure and potential energy

The pair distribution function $g(r)$ is the probability of finding a pair of particles at a distance r. Usually, $g(r)$ is used to characterize the structure of random systems. On the other hand, the average potential energy per particle u is determined by the interactions among the particles composing the system, so u depends upon the structure of the system. To find the relationship between u and g, we investigated the variation of g and u with time t in the gas–liquid phase separation process by MD simulations. We are interested in the liquid-like clusters which are generated during phase separation. The average size of the clusters can to some extent be characterized by the average number of nearest-neighbour particles, n_{nn}, which is the number of particles within a distance corresponding to the first minimum of $g(r)$. With the advance of time, the clusters grow and n_{nn} rises. As n_{nn} increases, more particles aggregate together, so u reduces. Our MD simulations have shown that u and n_{nn} behave similarly with the variation of time. Figure 1(a) presents the evolution of $u(t)$ and $n_{nn}(t)$ with time t. Figure 1(b) plots the relation between $u(t)$ and $n_{nn}(t)$.

It can been seen from figure 1(b) that a very good linear relation between $u(t)$ and $n_{nn}(t)$ is obtained except in about the first 40 MDs. The linear relation between $u(t)$ and $n_{nn}(t)$ can be deduced as follows. From the pair distribution function $g(r, t)$, the average potential energy per particle $u(t)$ can be expressed as

$$u(t) = \pi\rho \int_0^\infty \phi(r)g(r,t)r \, dr = \pi\rho \int_0^{r_{cut}} \phi(r)g(r,t)r \, dr \tag{3}$$

and the average number of nearest-neighbour particles $n_{nn}(t)$ as

$$n_{nn}(t) = 2\pi\rho \int_0^{r_1} g(r,t)r \, dr \tag{4}$$

where $\rho = \rho_c$ is the mean density of the system and r_1 corresponds to the first minimum in the pdf $g(r)$.
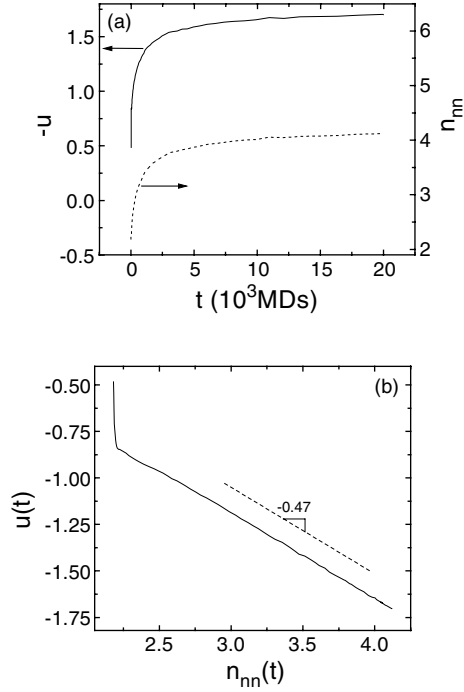
Figure 1. Plots at phase separation temperature $T = 0.45$ and critical density $\rho_c = 0.325$: (a) the evolution of the average potential energy per particle u (solid line) and the average number of nearest-neighbour particles n_{nn} (dashed line) with time t; (b) the dependence of $u(t)$ on $n_{nn}(t)$.

Equations (3) and (4) can be combined into

$$u(t) = k(t)n_{nn}(t) \tag{5a}$$

where

$$k(t) = \left(\int_0^{r_{cut}} \phi(r)g(r,t)r \, \mathrm{d}r \right) \bigg/ \left(2 \int_0^{r_1} g(r,t) \, \mathrm{d}r \right). \tag{5b}$$

After a brief time, the separation process reaches a situation in which small liquid clusters are formed whose internal structure is already equivalent to that of the equilibrium liquids. This can also be indicated indirectly by the invariance of the positions of liquid peaks in $g(r,t)$. In this case, the time- and distance-dependent $g(r,t)$ can be expressed as [1]

$$g(r,t) = G_{max}(t)\tilde{g}(r) \tag{6}$$

where $G_{max}(t)$ is a function of time only and $\tilde{g}(r)$ is a function of distance. $G_{max}(t)$ represents the magnitude factor of $g(r,t)$ concerned with the average cluster size of the system, while $\tilde{g}(r)$ denotes the shape factor relating to the internal structure of liquid-like clusters. Inserting equation (6) into equation (5b), we obtain the time-independent

$$k_0 = \left(\int_0^{r_{cut}} \phi(r)\tilde{g}(r)r \, \mathrm{d}r \right) \bigg/ \left(2 \int_0^{r_1} \tilde{g}(r) \, \mathrm{d}r \right). \tag{7}$$

Employing equation (7), equation (5a) can be rewritten as

$$u(t) = k_0 n_{nn}(t). \tag{8}$$

It just describes the behaviour of $u(t)$ with $n_{nn}(t)$ in figure 1(b). By taking any $g(r,t)$ for $t > 40$ MDs as $\tilde{g}(r)$, we calculate the value of $k_0 = -0.47 \pm 0.02$, which is in agreement with the simulation results in figure 1(b).

3.2. Evolution of potential energy with time

Since the evolution of the average potential energy per particle $u(t)$ reflects the growth of liquid-like clusters in the separation process, one may investigate the gas–liquid phase separation process, especially in the early times, using $u(t)$ instead of the direct structure description. Figure 2 shows the variation of the average potential energy per particle $u(t)$ and the average excess energy per particle $u(t) - u_\infty$ with time in a log–log plot at quenched temperature $T = 0.45$, respectively. $u_\infty \simeq -1.81$ is the average potential energy per particle of coexisting phases at equilibrium, where the phases are separated by a flat interface.
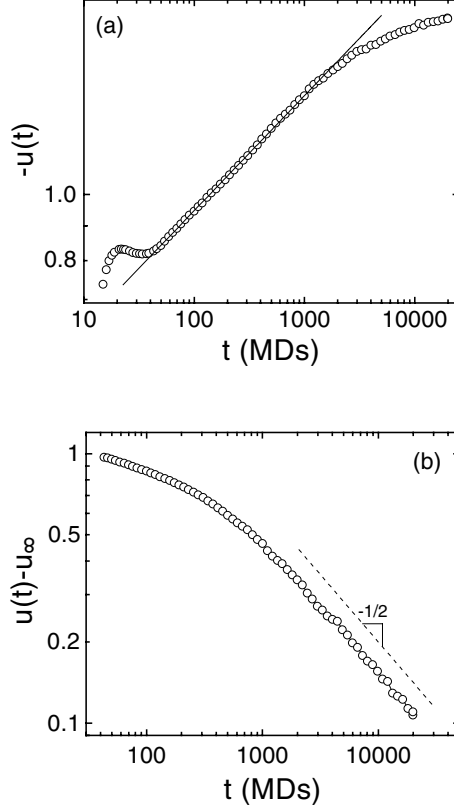

Figure 2. For the same conditions as for figure 1: (a) the evolution of the average potential energy per particle $u(t)$ versus time t in a log–log plot (the solid line is to guide the eye); (b) the dependence of the excess internal energy $u(t) - u_\infty$ on time in a log–log plot.

Figure 2(a) shows that after a microscopic time t_{mic} (40 MDs), $u(t)$ follows a positive power law in the early stage of phase separation ($40 < t < 1000$ MDs), i.e.

$$u(t) \propto t^\theta \tag{9}$$

and figure 2(b) indicates that there exists a negative power relation between the excess energy and time in the late stages ($t > 5000$ MDs), i.e.

$$u(t) - u_\infty \propto t^{-x}. \tag{10}$$

The intermediate range ($1000 < t < 5000$ MDs) is the crossover region between the early and late stages.

The result of equation (10) is consistent with those in previous works [7, 11], i.e. x in equation (10) is the same as α in $R(t) \sim t^{\alpha}$, which has been demonstrated and explained on the basis of the cluster dynamics in the late stage of phase separation [1, 11]. Therefore, in the following we will discuss the early-time behaviours of $u(t)$ on the basis of cluster dynamics only.

We calculated the total potential energy U_l of a cluster consisting of l particles at different times. The cluster potential energy U_l as a function of cluster size l is shown in figure 3 in a log–log plot for an extensive time range from 200 to 20 000 MDs. It can be found from figure 3 that U_l approximately follows a power law in the cluster size l:

$$U_l = Al^{\beta}. \tag{11}$$

where β is an universal exponent. We obtained $\beta = 1.13 \pm 0.02$ from figure 3. A is a pre-exponential factor, which depends on the temperature of phase separation but does not depend on the time. From figure 3 we obtained $A = 0.65 \pm 0.06$.
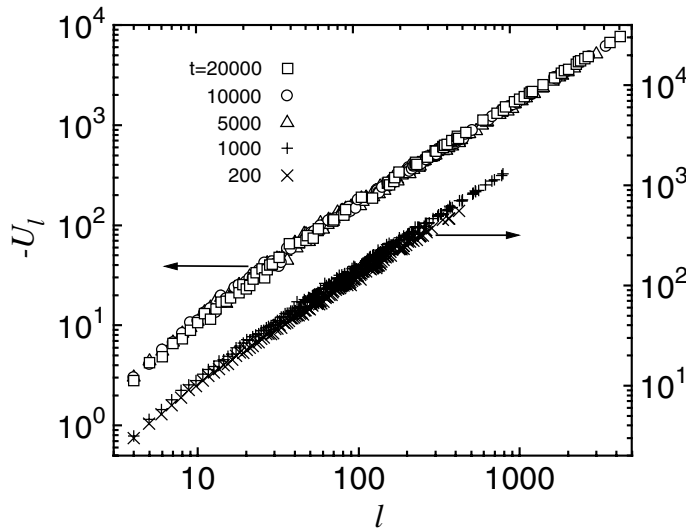

Figure 3. For the same conditions as for figure 1: the total potential energy U_l of a cluster consisting of l particles as a function of cluster size l in a log–log plot in an extensive time region from 200 to 20 000 MDs.

To establish in which time region equation (11) is suitable for the cluster description of phase separation, we examined the relative error $\delta U/U$ of the total potential energy of the system between the MD simulation and equation (11):

$$\frac{\delta U}{U}(t) = \left| \left(\sum_l U_l n_l(t) - \sum_l U_l^{\text{MD}} n_l(t) \right) \middle/ \left(\sum_l U_l^{\text{MD}} n_l(t) \right) \right| \tag{12}$$

where $n_l(t)$ is the number of clusters with l particles at time t. We found that $\delta U/U$ is very small in the early stage ($\delta U/U < 1\%$). As time increases, $\delta U/U$ becomes larger and larger, and reaches 15% after 5000 MDs. It follows from this that equation (11) describes the behaviour of the clusters dynamics accurately in the early stage of phase separation, but generates a large error in the late stage.

For the systems undergoing first-order phase transitions, the dynamical theory of cluster formation has been developed by Binder *et al* [1]. A general kinetic equation for $n_l(t)$ has

been obtained [1]:

$$\frac{\partial n_l(t)}{\partial t} = \frac{\partial}{\partial l}\left(R_l n_l \frac{\partial}{\partial l}\frac{n_l(t)}{n_l}\right) + \frac{1}{2}\int_{l_c}^{l} \mathrm{d}l'\, W(l-l',l')\frac{n_{l'}(t)}{n_{l'}}\frac{n_{l-l'}(t)}{n_{l-l'}}$$
$$- \frac{n_l(t)}{n_l}\int_{l_c}^{\infty} \mathrm{d}l'\, W(l,l')\frac{n_{l'}(t)}{n_{l'}} \tag{13}$$

where the kinetic coefficient R_l is

$$R_l = \frac{1}{n_l}\sum_{l'=1}^{l_c}(l')^2 W(l-l'). \tag{14}$$

n_l is the equilibrium cluster distribution, $W(l,l')$ is a rate relating to clusters with size l and l', and l_c is a cut-off such that the volume V_{l_c} associated with the correlation length of the system ξ is $V_{l_c} \sim \xi^d$. The first term in equation (13) is the Becker–Döring nucleation equation [1]. The last two terms correspond to the standard coagulation equation [1].

To obtain the cluster distribution in the early stage of phase separation, we introduce an approximate solution of equation (13) which yields the phenomenological Binder–Stauffer (BS) theory of cluster growth at intermediate times [1]. Their basic assumption is that there exists an intermediate time domain in which clusters of intermediate size diffuse without changing size, until eventually two such clusters coalesce. This coagulation is the BS growth mechanism and results from the diffusion of clusters. The clusters are considered to be diffusing, free Brownian particles. Based on the assumptions above, the BS theory can be derived from the basic equation (13) as follows. We neglect the evaporation–condensation term in equation (13) (the first term) and keep the coagulation terms. A scaling form for the rate $W(l,l')$ is then assumed for the coagulation terms in equation (13):

$$W(l,l') = n_l n_{l'} l'^v \tilde{W}(l/l'). \tag{15}$$

With this form of W and the conservation law $\sum_l n_l(t)l = \text{constant}$, the equation for $n_l(t)$ can be solved by the following scaling form [1]:

$$n_l(t) = t^z \tilde{n}(\xi) \tag{16}$$

with

$$y = -z/2 = (1-v)^{-1} \tag{17}$$

where $\xi = lt^{-y}$ and $\tilde{n}(\xi)$ is an appropriate scaling function. The exponent v is obtained according to the diffusion of the clusters. y has at least three different values: $d/(d+1)$, $d/(d+2)$, and $d/(d+3)$, corresponding to three different diffusion mechanisms [1]. Note that the scaling solution, equation (16), was originally proposed for the late stage of phase separation of the Lifshitz–Slyozov (LS) theory [1]. However, in contrast to the BS theory, the LS theory results from neglecting the coagulation events (the last two terms) in equation (13) and also neglecting the diffusion part ($\partial^2/\partial l^2$) of the evaporation–condensation term (the first term). Therefore, in the LS theory, the exponent $y = d/3$ is universal (independent of temperature, etc) [1].

Now we use the BS theory to discuss our simulation results at intermediate times ($40 < t < 1000$ MDs). Combining equations (11) and (16), the average potential $u(t)$ is expressed as

$$u(t) = \frac{1}{N}\sum_l U_l n_l(t) = t^{z+y+\beta y}\frac{1}{N}\sum_\xi A\xi^\beta \tilde{n}(\xi). \tag{18}$$

Substituting the relation $z = -2y$ into equation (18), we obtain

$$u(t) = A't^{(\beta-1)y} \tag{19}$$

where $A' = \sum_\xi A\xi^\beta \tilde{n}(\xi)/N$. Equation (19) describes the evolution of the average potential energy per particle with time in the early stage of phase separation (see figure 2(a)). Comparing equations (9) and (19), we obtain

$$\theta = (\beta - 1)y. \tag{20}$$

Since y is not universal in the BS mechanism [1], one can except θ to depend on the phase separation temperature. Figure 4 demonstrates that for the simulations carried out at different quenched temperatures this is the case. From figure 4, we obtain $\theta \simeq 0.195, 0.156$, and 0.130 for quenched temperatures $T = 0.40, 0.45$, and 0.50, respectively. Substituting these values of θ into equation (20), we obtain $y \simeq 1.5, 1.2$, and 1.0 for quenched temperatures $T = 0.40$, 0.45, and 0.50, respectively.
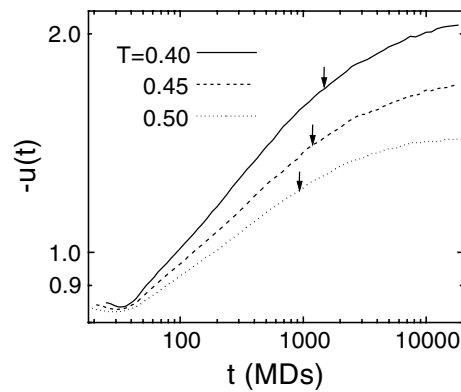

Figure 4. The evolution of the average potential energy per particle $u(t)$ with time t in a log–log plot at different quenched temperatures. The crossover times are indicated by arrows.

It can be seen that our simulation results for y are different to those obtained from the BS theory. This may result from the BS theory only being suitable for describing systems with nearest-neighbouring interactions at low temperatures; this limitation is imposed by its basic assumptions [1]. In the present system the interaction is not limited to the nearest neighbours and has a more extensive range. That is, during the diffusion a cluster has interactions with its surrounding clusters and the clusters cannot be regarded as free Brownian particles. Therefore, the value of v in the present systems is different from that in the BS theory. In addition, the probability of sticking of two neighbouring clusters $P(l, l')$ is always less than 1.0, and increases with decreasing temperature. Therefore, the rate $W(l, l')$ should be dependent not only on the diffusion of clusters (reflected by v), but also on the probability $P(l, l')$, i.e.

$$W(l, l') = n_l n_{l'} l'^v P(l, l') \tilde{W}(l/l'). \tag{21}$$

Accordingly, although the form of the solution equation (16) does not change, two basic assumptions in the BS mechanism are no longer satisfied in the present systems, so the values of y obtained from the present simulations are very different from those obtained from the BS theory. In the following, we discuss the dependence of our simulation results on the phase separation conditions.

With the phase separation temperature decreasing, the influence of thermal fluctuation becomes small, and the movement of clusters is more directional because of the long-range interaction between clusters. Consequently, the average distance over which clusters diffuse before coalescing becomes smaller and the exponent v becomes larger [1]. Moreover, the sticking probability $P(l, l')$ increases with decreasing temperature. Therefore, the exponent

y, which reflects the cluster growth velocity, increases with reducing temperature. This is qualitatively consistent with our simulation results.

When the temperature is sufficiently low, the sticking probability $P(l, l')$ approximates to 1.0, and equation (21) reduces to equation (15). Since the thermal fluctuations are very small at low temperatures, the movement of clusters is governed by the interactions between clusters. The interactions mainly result from the surface particles of clusters, so the interactions are approximately proportional to the surface area of the clusters. Therefore, we may make the single assumption that the rate W is proportional to the surface area of the clusters S, i.e. $W \propto S \sim l^{1/2}$, so $v = 1/2$. Combining this with equation (17), we obtain $y = 2.0$. That is, the exponent y tends to 2.0 with decreasing temperature, which is in agreement with the present simulation results for y.

From figure 4 we can also see that the curves have similar behaviours with time. For each quenched temperature, there exists a crossover time t_ξ. For $t_{mic} < t < t_\xi$, $u(t)$ is expressed by using equation (9), and for $t \gg t_\xi$, $u(t)$ can be expected to follow equation (10).

In addition, in order to check the effect of the initial conditions on simulation results, we elevated the initial equilibrium temperatures ($T = 6.0, 7.0$, and 8.0) of the simulation system. The results obtained are almost the same. To examine the effect of finite size on simulations, we took three systems with $N = 2000, 3000$, and 4000, and found that the simulation results are insensitive to the size of the systems.

4. Conclusions

This work shows that the average potential energy per particle $u(t)$ can be used to describe the process of gas–liquid phase separation. The results also show that at early times the potential energy per particle follows a positive power law of time after a microscopic time. Unlike in the late stage, the power-law exponent is not universal and is dependent on the phase separation temperature. On the basis of cluster dynamics, we explain the power-law behaviour in the early stage and discuss the dependence of the exponent on the temperature.

Acknowledgments

References

[1] Gunton J D, Miguel M S and Sahni P S 1983 *Phase Transitions and Critical Phenomena* vol 8, ed C Domb and J L Lebowitz (London: Academic)
[2] Binder K 1987 *Rep. Prog. Phys.* **50** 783
[3] Rovere M, Heermann D W and Binder K 1990 *J. Phys.: Condens. Matter* **2** 7009
[4] Ten Wolde P R and Frenkel D 1997 *Science* **277** 1975
[5] Ten Wolde P R and Frenkel D 1998 *J. Chem. Phys.* **109** 9901
      Ten Wolde P R and Frenkel D 1998 *J. Chem. Phys.* **109** 9919
[6] Velasco E and Toxvaerd S 1994 *J. Phys.: Condens. Matter* **6** A205
[7] Velasco E and Toxvaerd S 1996 *Phys. Rev.* E **54** 605
[8] Taneike T and Shiwa Y 1999 *J. Phys.: Condens. Matter* **11** L147
[9] Tanaka H 2000 *J. Phys.: Condens. Matter* **12** R207
[10] Bock H and Schoen M 2000 *J. Phys.: Condens. Matter* **12** 1569
[11] Schöbinger M, Koch S W and Abraham F F 1986 *J. Stat. Phys.* **42** 1071
[12] Gonnella G, Orlandini E and Yeomans J M 1999 *Phys. Rev.* E **59** R4741
[13] Bray A J 1994 *Adv. Phys.* **43** 357

[14] Lifshitz I M and Slyozov V V 1961 *J. Phys. Chem. Solids* **19** 35
[15] Lookman T, Wu Y, Alexander F J and Chen S 1996 *Phys. Rev.* E **53** 5513
[16] Mauri R, Shinnar R and Triantafyllou G 1996 *Phys. Rev.* E **53** 2613
[17] Oono Y and Puri S 1988 *Phys. Rev.* A **38** 434
     Oono Y and Puri S 1988 *Phys. Rev.* A **38** 1542
[18] Bastea S and Lebowitz J L 1995 *Phys. Rev.* E **52** 3821
[19] Alexander F, Chen S and Guanau D W 1993 *Phys. Rev.* B **48** 634
[20] Kendon V M, Desplat J C, Bladon P and Cates M E 1999 *Phys. Rev. Lett.* **83** 576
[21] Zhang W B, Zou X W, Jin Z Z and Tian D C 1999 *Physica* A **272** 12
[22] Koch S W, Desai R C and Abraham F F 1983 *Phys. Rev.* A **27** 2152
[23] Yamamoto R and Nakanishi K 1994 *Phys. Rev.* B **49** 14 958
     Yamamoto R and Nakanishi K 1995 *Phys. Rev.* B **51** 2715
[24] Desai R C and Denton A R 1986 *On Growth and Form* ed H E Stanley and N Ostrowsky (The Hague: Nijhoff)
[25] Butler B D, Hanley H J M, Hamsen D and Evans D J 1995 *Phys. Rev. Lett.* **74** 4468
[26] Klein W 1990 *Phys. Rev. Lett.* **65** 1462
[27] Zhang W B, Zou X W, Jin Z Z and Tian D C 2000 *Phys. Rev.* E **61** 2805
[28] Furukawa H 1997 *Phys. Rev.* E **55** 1150
[29] Velasco E and Toxvaerd S 1993 *Phys. Rev. Lett.* **71** 388
[30] Laradj M, Toxvaerd S and Mouritsen O 1996 *Phys. Rev. Lett.* **77** 2253
[31] Ossadnik P, Gryre M F, Stanley H E and Glotzer S 1994 *Phys. Rev. Lett.* **72** 2498
[32] Leptoukh G, Strickland B and Roland C 1995 *Phys. Rev. Lett.* **74** 3636
[33] Nosé S 1984 *Mol. Phys.* **52** 255
     Hoover W G 1985 *Phys. Rev.* A **31** 1695
[34] Barker J A, Henderson D and Abraham F F 1981 *Physica* A **106** 226